



# Polypropylene nonwoven fabric modified with oxime and guanidine for antibiofouling and highly selective uranium recovery from seawater

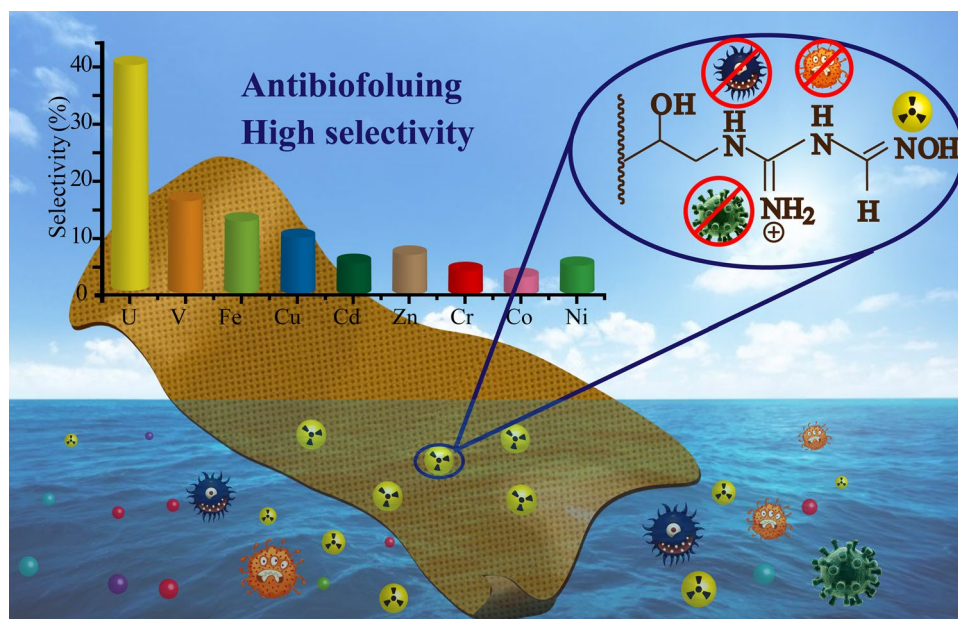
Sen Yang<sup>1</sup> · Guoxun Ji<sup>2</sup> · Suya Cai<sup>1</sup> · Meiyu Xu<sup>1</sup> · Daoben Hua<sup>1,3</sup>

Received: 26 March 2019 / Published online: 28 May 2019  
© Akadémiai Kiadó, Budapest, Hungary 2019

## Abstract

A novel adsorbent for antibiofouling and highly selective uranium recovery from seawater is developed in this work. Specifically, the polypropylene nonwoven fabric modified with oxime and guanidine was obtained by subsequent radiation-grafting, ring-opening and oximation reaction. The adsorbent demonstrates outstanding selectivity for uranium(VI) against other competing metal ions in real seawater. The antibacterial assay indicated the adsorbent has good antibacterial properties against *Escherichia coli* and *Staphylococcus aureus*. XPS spectra indicate that uranium(VI) is adsorbed on the non-woven through the interaction with multiple groups. This work shows that the sorbent may be a hopeful material for the extraction of uranium from seawater.

## Graphical abstract



**Keywords** Adsorption · Uranium · Oxime · Antibiofouling · Seawater

**Electronic supplementary material** The online version of this article (<https://doi.org/10.1007/s10967-019-06578-7>) contains supplementary material, which is available to authorized users.

Extended author information available on the last page of the article

## Introduction

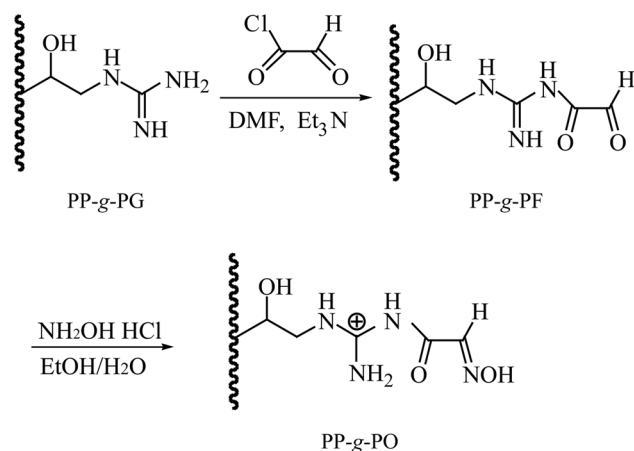
The increasing demand for uranium makes people's attention turn to the ocean with the expansion of nuclear industry in the world. There are  $4.5 \times 10^9$  tons of uranium in seawater, which is about 1000 times that on land and could be used to supply nuclear energy for thousands of years [1, 2]. In addition, extracting of uranium from seawater can potentially reduce the environmental problems caused by mining of radioactive and toxic uranium on land [3, 4]. However, there is still a huge challenge to extract uranyl ions efficiently from seawater attributed to the low uranium(VI) concentration in seawater, the existence of many coexisting ions, and biofouling. Therefore, the development of economical and efficient uranium recovery materials is of great significance for the continuous supply of nuclear energy in the future.

In recent years, various materials have been developed for uranium extraction, such as membrane material [5], porous carbon [6, 7], iron tetraoxide [8], graphene [9], porous aromatic frameworks [10, 11], and fiber materials [12–15]. Besides, nano quantum dots [16–18], small molecule [19], biomolecule [20], fluorescent polymer [21] have been used for uranium detection. Among them, polyamidoxime-based fiber adsorbents have been extensively studied for uranium extraction due to the strong coordination with uranyl ions and good mechanical stability, easy recycling, and operability of fiber materials. For instance, Das et al. [14] developed amidoxime functional polyethylene non-woven fabric by irradiation grafting with a extraction capacity of 3.35 mg U/g after 8 weeks of marine tests in the Pacific Northwest National Laboratory of the United States. Dai et al. [22] prepared tert-butyl acrylate and amidoxime functionalized polyvinyl chloride fibers, and the adsorption capacity of the adsorbent was as high as 5.22 mg/g after sea-test for 49 days. However, polyamidoxime-based sorbents showed a stronger affinity for vanadium(V) with a sorption capacity approximately 5 times more than that for uranium(VI) [14]. Rao et al. [23, 24] conducted in-depth studies on the coordination mechanism of amidoxime with vanadium(V) and uranium(VI), and found that the open-chain amidoxime group do not bind with vanadium(V), and a non-oxido  $V^{5+}$  complex was formed with the cyclic imide-dioxime group, while both groups have strong affinity with uranium(VI). In addition, the coordination mode between the open chain amidoxime group and uranium(VI) is  $\eta^2$  type through the N and O atoms of the oxime group [12, 25]. Therefore, in order to avoid ring formation of amidoxime with good coordination ability for vanadium(V), an oxime-based adsorbent with highly selectivity for uranium(VI) can be expected. Xu et al. [26] synthesized polyoxime-functionalized magnetic

nanoparticles for the selective adsorption of uranyl ions, and found that the selectivity of polyoxime-based adsorbents for uranium(VI) was significantly higher than that of vanadium(V) and other competing ions. However, nano-materials are difficult to use in real seawater environments, which greatly limits their application.

Recently, biofouling effects of the sorbents have been noticed for extracting uranium from seawater. Wu et al. [27] studied amidoxime modified polyethylene fiber for the extraction of uranium(VI) from seawater, and found that massive sediment and marine life were observed on the surface of the fibers after 42 days of marine tests in the China East Sea, which hindered the full contact between ligands and uranyl ions. Park et al. [28] found that the adsorption capacity of sorbents for uranium decreased by 30% under light irradiation, and a large number of algal cells were observed by microscope after 42 days, and concluded that it may be necessary to use adsorbents in deep marine environments in order to reduce biofouling effects. However, it will undoubtedly increase operating costs. Therefore, it is significant to develop anti-biofouling adsorbents to improve the economic efficiency of uranium extraction from seawater. We recently reported a guanidine-functionalized polypropylene non-woven fabric to solve the problem of biofouling of uranium extraction from seawater for the first time [29]. The guanidine group in the material can effectively inhibit the adhesion of *E. coli* by destroying the cytoplasmic phospholipid membrane of the bacterial cells to the death of the bacteria [30]. Wen et al. [31] prepared nano  $TiO_2$  and amidoxime-modified wool fiber composite by in situ deposition for uranium(VI) recovery, the sorbent displayed good antibacterial property due to the presence of  $TiO_2$ . Zhang et al. [32] synthesized poly-dopamine and Ag nanoparticles functionalized activated carbons for uranium(VI) sorption from simulated seawater with an antifouling feature. Despite some explorations have been made in the field of antibiofouling, the selectivity of these materials for uranium(VI) needs to be further improved. Therefore, it is still of great significance to develop new adsorbents with both antibiofouling property and high selectivity for uranium(VI) in practical application.

In this paper, a new adsorbent is reported for uranium(VI) recovery from seawater. Specifically, polypropylene nonwoven fabric was functionalized with the oxime and guanidine groups by the subsequent reactions (Scheme S1, Supporting Information; Scheme 1). The combination of oxime with guanidine groups will endow the adsorbent with the high selectivity and good anti-biofouling properties. Therefore, it is expected that the new adsorbent could achieve efficient enrichment of uranium in seawater.



**Scheme 1** Schematic for preparation of polypropylene nonwoven fabric modified with oxime and guanidine (PP-g-PO)

## Experimental

### Materials and reagents

PP nonwoven fabric ( $85 \text{ g/m}^2$ ) was purchased from Kingway Complex Material Co., Ltd., Nantong, China. Glycidyl methacrylate (GMA, CP), triethylamine ( $\text{Et}_3\text{N}$ , AR), hydroxylamine hydrochloride (CP), thionyl chloride (CP) and *N,N'*-Dimethylformamide (DMF, AR) were bought from Sinopharm Chemical Reagent Co., Ltd, Shanghai, China. Glyoxylic acid monohydrate (98%) was purchased from Adamas Reagent Co., Ltd., Shanghai, China.  $\text{UO}_2(\text{NO}_3)_2 \cdot 6\text{H}_2\text{O}$  (AR) was purchased from Sigma Aldrich Fluka, St. Louis, United States. Sea water was obtained from Bohai, Qingdao, China, and filtered prior to use. The strains of *E. coli* (ATCC 11229) and *S. aureus* (ATCC 6538) were acquired from Hygia Biotech Co., Ltd, Suzhou, China.  $\text{Et}_3\text{N}$  was dried over 4A molecular sieves. Characterization methods and synthesis of PP-g-PG are shown in Supporting Information.

### Synthesis of functional polypropylene nonwoven fabric (PP-g-PO)

Formyl group functionalized non-woven fabric (PP-g-PF) were prepared according to the modified literature process [26]. Specifically, the guanidine modified polypropylene non-woven fabric (PP-g-PG) (1.0 g) was immersed in a mixed solvent of anhydrous DMF (20 mL) and anhydrous  $\text{Et}_3\text{N}$  (8 mL, 30.9 mmol). 2-Oxoacetyl chloride (2.4 g, 25.9 mmol) in 20 mL anhydrous DMF was added into the PP-g-PG dispersion at  $25^\circ\text{C}$ . Then, the mixture was reacted under magnetic stirring at  $100^\circ\text{C}$  for 20 h in argon ambience. After cooling it to about  $25^\circ\text{C}$ , the fiber material was rinsed with DMF and ultrapure water three times, and then dried to obtain the PP-g-PF.

The aldehyde on PP-g-PF was treated with hydroxylamine hydrochloride and converted to oxime group. Typically, hydroxylamine hydrochloride (1.0 g, 14.4 mmol) was dissolved in water/methanol (40 mL, v/v = 1:1; pH ~ 7.0), followed by the addition of PP-g-PF (1.0 g) into the solution. The oximated sorbent was washed with ultrapure water/methanol (v/v = 1: 1) for 3 times after refluxing for 8 h at  $80^\circ\text{C}$ , and then desiccated to give PP-g-PO.

### Sorption experiments

The sorbent (10 mg) was added into  $2 \times 10^{-5} \text{ mol/L}$  uranium(VI) solution (40 mL), and shaken at room temperature until the adsorption equilibrium. Uranium(VI) solutions were gained by dissolving  $\text{UO}_2(\text{NO}_3)_2 \cdot 6\text{H}_2\text{O}$  in ultrapure water and the pH was adjusted to  $8.0 \pm 0.1$  by  $\text{Na}_2\text{CO}_3$  solution (2 mol/L). The concentrations of uranium before and after sorption were quantified by ICP-MS. The sorption amount ( $q_e$ , mg/g) and sorption efficiency (SE) were obtained according to Eqs. (1) and (2), respectively:

$$q_e = (C_0 - C_e) \frac{V}{M} \quad (1)$$

$$\text{SE} (\%) = \frac{C_0 - C_e}{C_0} \times 100 \quad (2)$$

where  $C_0$  is the initial concentrations of uranium,  $C_e$  (mg/L) is the residual uranium concentrations,  $V$  (L) is the volume of aqueous solution, and  $M$  (g) is the sorbent mass.

### Desorption and regeneration experiments

The reusability of PP-g-PO was evaluated through 5 sorption–desorption cycles. In each cycle, PP-g-PO (10 mg) was immersed in  $2 \times 10^{-5} \text{ mol/L}$  uranium(VI) solution (40 mL), and shaken for 4 h at 298.15 K, then the PP-g-PO combined with uranium(VI) was desorbed by stirring in eluents (3 mol/L  $\text{KHCO}_3$  at  $40^\circ\text{C}$  and 0.1 mol/L HCl at  $25^\circ\text{C}$ ) for 3 h after rinsed with 50 mL ultrapure water for three times. The fabric was washed with 50 mL ultrapure water for three times after the elution, and then desiccated for reuse.

### The real seawater tests

The real seawater from Bohai was used to study the selectivity of uranium onto PP-g-PO. The sorbent (3.0 mg) was added into real seawater (5.0 L) and shaken for 23 days at 298.15 K. After the dissolution of the uranyl-adsorbed PP-g-PO solid in 4 mL of  $\text{HNO}_3$  and 1 mL  $\text{H}_2\text{O}_2$  (30%), the adsorption capacity for the ions were determined according to the ICP-MS. Uranium selectivity ( $S_U$ ) was used to

describe the selectivity of sorbents for uranium in real seawater, and it was obtained according to Eq. (3): [33]

$$S_U(\%) = \frac{q_{e-U}}{q_{e-tot}} \times 100 \quad (3)$$

where  $q_{e-U}$  is the sorption amount for uranium (mg/g) and  $q_{e-tot}$  is the sorption amount for total cations (mg/g).

## Antibacterial assay

The antibacterial assay was conducted according to the modified literature method [34]. The antibiofouling and bactericidal properties of PP-g-PO were studied using Gram-negative *E. Coli* and Gram-positive *S. aureus*, respectively. Firstly, *E. Coli* and *S. aureus* cells were inoculated at 37 °C for 24 h. Single colonies were removed and incubated in 50 mL of liquid medium for 24 h, and the supernatant was removed by centrifugation for 10 min (3000 rpm). Dilute the colonies to the appropriate concentration with PBS. Finally, 600  $\mu$ L of the bacterial solution ( $\sim 1 \times 10^6$  CPU) was placed in a 24-well plate, and the original polypropylene non-woven fabric or modified fabric was put in the well and hatched at 37 °C for 24 h. The non-woven fabric was taken out, rinsed several times with PBS, and then fixed with paraformaldehyde (4%) for 10 min. Finally, dehydration was carried out for 30 min with a mixture of ethanol/ultra-pure water having a volume fraction of 10, 30, 50, 70 and 100%, and then dried under vacuum at 50 °C.

## Results and discussion

### Characterization of PP-g-PO

The chemical components of the resultant sorbents were confirmed by FT-IR and XPS. As shown in Fig. 1, the appearance of stretching vibrations peak of C=O at 1724  $\text{cm}^{-1}$  and C–O ring at 904  $\text{cm}^{-1}$  in the spectra of PP-g-PGMA (Fig. 1A, trace b) in comparison with unmodified fabric (Fig. 1A, trace a) demonstrated PGMA was immobilized onto the non-woven fabric material [35]. In addition, the stretching vibrations of N–H (3362  $\text{cm}^{-1}$ ), C=N, CH=O (1655  $\text{cm}^{-1}$ ), and C–N (1046  $\text{cm}^{-1}$ ) of PP-g-PG indicated that the epoxy in PP-g-PGMA has successfully reacted with guanidine hydrochloride [36]. After the amino group of PP-g-PG was reacted with 2-oxoacetyl chloride, the characteristic peak of PP-g-PF remained (C=O peak at 1724  $\text{cm}^{-1}$ ). After further oximation, the N–O peak at 937  $\text{cm}^{-1}$  was appearance, which was further characterized by XPS (Fig. 1D).

As shown in Fig. 1B, the O 1s characteristic peak appeared on the full spectrum of PP-g-PGMA compared with the original non-woven fabric (Fig. 1B, line a),

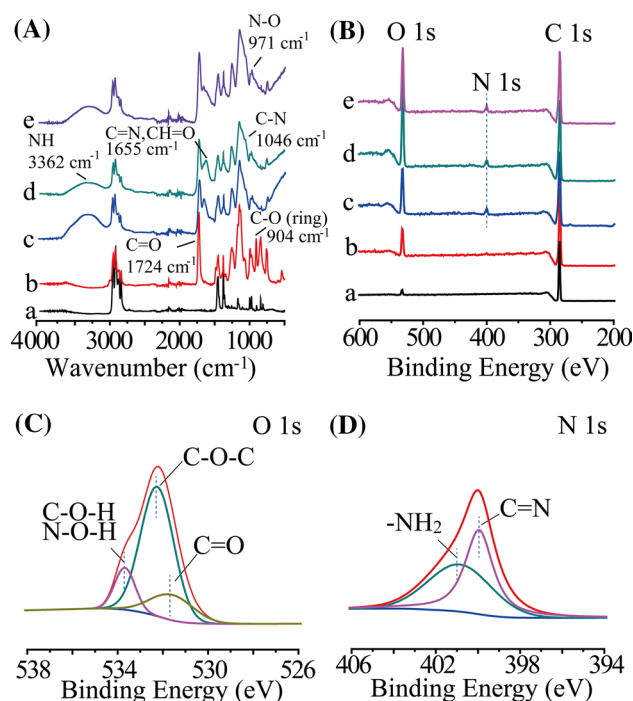


**Fig. 1** **A** FT-IR spectra of (a) PP non-woven fabric, (b) PP-g-PGMA, (c) PP-g-PG, (d) PP-g-PF and (e) PP-g-PO; **B** XPS spectra of (a) PP non-woven fabric, (b) PP-g-PGMA, (c) PP-g-PG, (d) PP-g-PF, (e) PP-g-PO, and XPS spectra of **C** O 1s, **D** N 1s of PP-g-PO

indicating that PGMA was successfully grafted onto the surface of PP nonwoven fabric (Fig. 1B, line b). After reaction with guanidine hydrochloride, 2-oxoacetyl chloride and oximation reaction, N 1s characteristic peaks appeared, indicating successful preparation of PP-g-PG, PP-g-PF and PP-g-PO (Fig. 2B, c, d and e lines). For PP-g-PO, the narrow spectrum of O 1s could be divided into three peaks attributing to C(N)–O–H, C–O–C, and C=O (Fig. 1C) while N 1s to –NH<sub>2</sub>, and C=N (Fig. 1D), which further proved the formation of oxime groups on the nonwoven fabric sorbent PP-g-PO. And the increase of N element on the surface of PP-g-PO further proved this point (Figure S1, Supporting Information).

The morphology of PP-g-PO was characterized by FESEM. As depicted in Fig. 2B, the fabric morphology remains intact after the reaction process. A distinct increase in average diameter of fibers was observed after functionalization compared with the original non-woven fabric (Fig. 2A), which was stemmed from the increasing of functional groups on the surface of fabric. Furthermore, the surface of the modified non-woven fabric PP-g-PO (Fig. 2D) is rougher than the original PP non-woven fabric surface (Fig. 2C), further indicating that the polymer is grafted on PP non-woven fabric.

The hydrophilic behavior of the fabrics was investigated through measuring the water contact angles, and the results

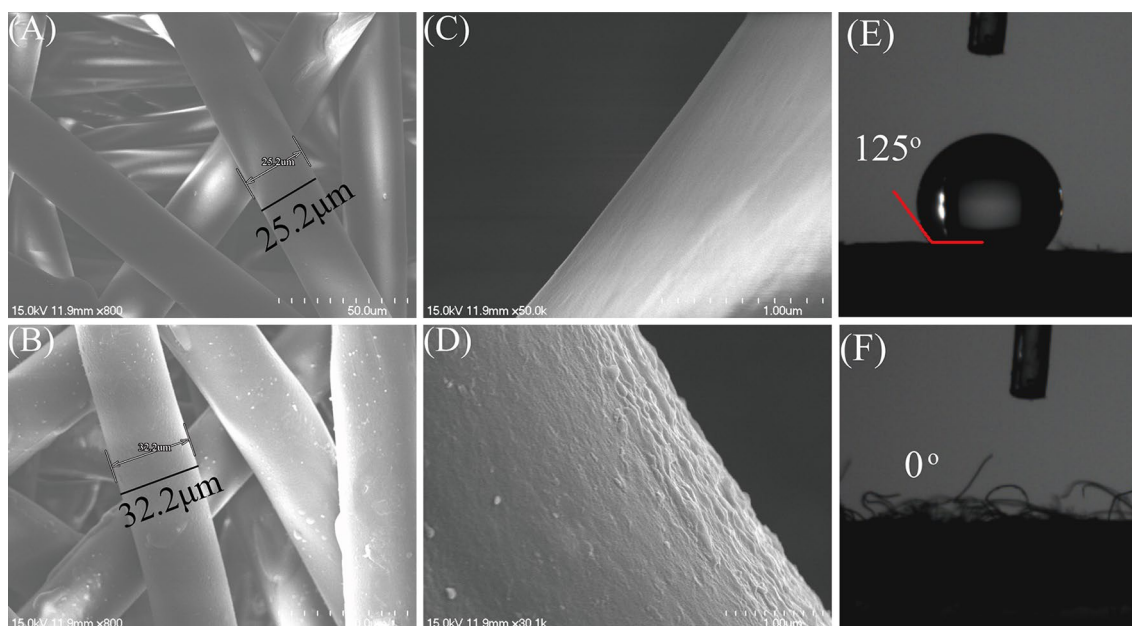


**Fig. 2** FE-SEM images of **A, C** PP nonwoven, **B, D** PP-g-PO. Scale bar: **A, B** 50.0  $\mu\text{m}$ , **C, D** 1.00  $\mu\text{m}$ . Water contact angles of **E** PP nonwoven and **F** PP-g-PO

were displayed in Fig. 2E, F. The unmodified PP non-woven fabric has a contact angle of  $125^\circ$  due to its inherent hydrophobicity (Fig. 2E). The modified non-woven fabric PP-g-PO, the contact angle dropped to  $0^\circ$  (Fig. 2F), indicating that the hydrophilic properties of the functionalized material were greatly improved.

### Sorption kinetics and isotherms

The adsorption kinetics experiment was carried out under the conditions of  $2 \times 10^{-5}$  mol/L uranyl ion concentration, 298.15 K and pH  $8.0 \pm 0.1$  with the optimum adsorbent dose of 0.25 g/L (Figure S2, Supporting Information). The correlation between adsorption time and capacity ( $q_t$ ) is shown in Fig. 3A. In the initial stage, the adsorption capacity of three sorbents increases rapidly with time and reaches the adsorption equilibrium within 4 h. Pseudo-first-order and pseudo-second-order models were employed to study the sorption kinetic (Figure S3, Supporting Information). The sorption process is more in line with pseudo-second-order model due to the larger correlation coefficients ( $R^2$ ) and the more accurate calculated  $q_e$  (Table 1). The  $k_2$  for PP-g-PO was much larger than that for PP-g-PF, implying the strong complexation between uranium(VI) and oxime. In the meantime, the  $k_2$  for PP-g-PG was larger than that for PP-g-PO, which may be attributed to the hydrophilia of guanidine on PP-g-PG, leading to a fast sorption. Furthermore, the sorption on PP-g-PO is faster than most of other fibrous materials (Table S1, Supporting Information), which may be ascribed to the strong coordination interaction between

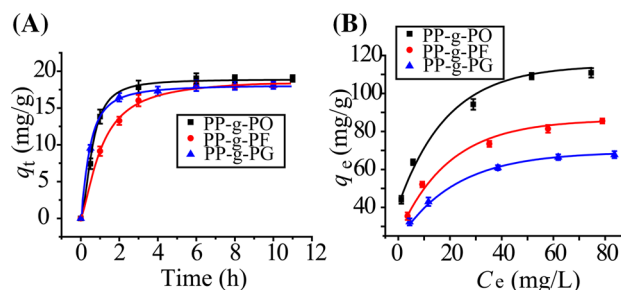


**Fig. 3** **A** Effect of contact time on the uranium(VI) sorption by PP-g-PO, PP-g-PF, and PP-g-PG. (Experimental condition: 10 mg sorbent dose, 40 mL solution,  $2 \times 10^{-5}$  mol/L uranium, pH  $8.0 \pm 0.1$ , and 298.15 K); **B** Sorption isotherm plots for uranium sorption by PP-g-PO, PP-g-PF, and PP-g-PG. (Experimental condition: 10 mg sorbent dose, 40 mL solution, pH  $8.0 \pm 0.1$ , and 298.15 K)

oxime and uranium and the hydrophilia of guanidine on the nonwoven fabric.

To evaluate the sorbent capacity of PP-g-PO, sorption isotherms researches were conducted by varying  $C_0$  of uranium(VI) ranged from 10 ppm to 100 ppm at 298.15 K and pH  $8.0 \pm 0.1$ . The correlation between  $q_e$  and  $C_e$  was displayed in Fig. 3B. Freundlich and Langmuir models were used to explain the sorption processes (Figure S4, Supporting Information), and the related parameters were listed in Table 2. The correlation coefficients ( $R^2$ ) fitted by Langmuir is relatively larger than that of Freundlich models, which is due to the uniform distribution of adsorption sites on the surface of materials, thus leading to monolayer sorption. Furthermore, the maximum capacity of PP-g-PO was calculated

**Table 1** Kinetic parameters for uranium sorption by PP-g-PO, PP-g-PF, and PP-g-PG (Experimental condition: 0.25 g/L sorbent dose, 40 mL solution,  $2 \times 10^{-5}$  mol/L uranium, pH  $8.0 \pm 0.1$ , and 298.15 K)

Sorbents	$q_{e, \text{exp}}$ (mg/g)	Pseudo-first order			Pseudo-second order		
		$k_1$ ( $\text{h}^{-1}$ )	$q_{e, \text{cal}}$ (mg/g)	$R^2$	$k_2$ (g/mg/h)	$q_{e, \text{cal}}$ (mg/g)	$R^2$
PP-g-PG	18.08	0.983	16.79	0.960	0.153	18.90	0.999
PP-g-PF	18.20	0.978	30.39	0.988	0.061	20.42	0.996
PP-g-PO	19.04	0.852	12.18	0.762	0.132	20.25	0.997

**Table 2** Parameters of Langmuir, Freundlich for uranium sorption by PP-g-PO, PP-g-PF, and PP-g-PG (Experimental condition: 0.25 g/L sorbent dose, 40 mL solution, pH  $8.0 \pm 0.1$ , and 298.15 K)

Sorbents	Langmuir			Freundlich		
	$q_{\text{max}}$ (mg/g)	$b$ (L/mg)	$R^2$	$K_F$ ( $\text{mol}^{1-n} \text{L}^n/\text{g}$ )	$n$	$R^2$
PP-g-PG	74.4	0.130	0.999	20.89	0.278	0.982
PP-g-PF	94.0	0.131	0.998	24.55	0.299	0.972
PP-g-PO	120.5	0.232	0.995	41.56	0.243	0.994

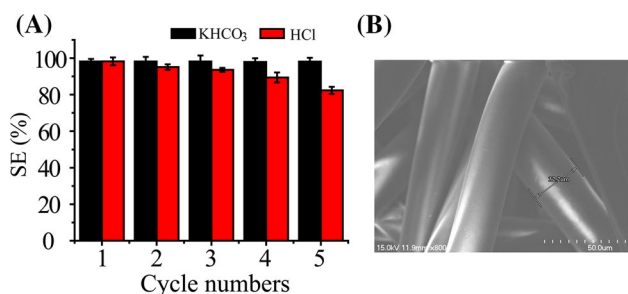


**Fig. 4** A Recycling of PP-g-PO for uranium sorption after five cycles, and B FE-SEM images of the PP-g-PO regenerated after five cycles. Scale bar: 50.0  $\mu\text{m}$ . (Experimental condition: 0.25 g/L sorbent dose, 40 mL solution,  $2 \times 10^{-5}$  mol/L uranium, pH  $8.0 \pm 0.1$ , and 298.15 K)

to be 120 mg U/g, which is a considerable value compared with the previous reported fibrous sorbents (Table S1, Supporting Information). Moreover, the equilibrium constant  $b$  value for PP-g-PO (0.232) was larger than that for PP-g-PG and PP-g-PF, which may be attributed to the stronger affinity between oxime and uranium(VI) [37].

### Desorption and regeneration studies

Sorption and desorption cycles were carried out for 5 times to study the regenerability of PP-g-PO with different eluates. The sorption efficiency (SE %) almost kept constant after five regeneration cycles using 3 mol/L  $\text{KHCO}_3$  as eluate (Fig. 4A), which may be ascribed to the formation of uranyl tris-carbonato complex at high bicarbonate concentrations [38]. In addition, there was no palpable damage to the surface of fibres by a FE-SEM image (Fig. 4B), which indicated the remarkable stability of bifunctional polypropylene non-woven fabric. However, the sorption efficiency descended to 80% by 0.1 mol/L HCl eluent. The similar results were obtained in other studies, which may be attributed to the deoximation under acidic solution [26, 39]. Therefore,

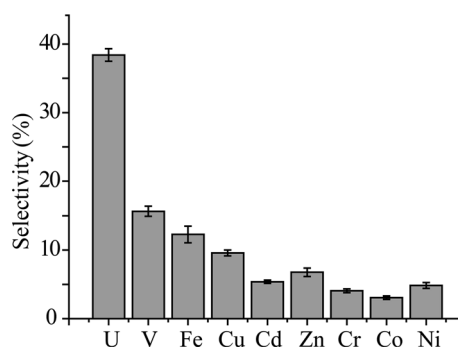


**Fig. 5** Sorption selectivity of PP-g-PO for metal ions in real seawater (Experimental condition: 3.0 mg sorbent dose, 5.0 L seawater, contact time = 23 d, pH 7.9, and 298.15 K)

3 mol/L  $\text{KHCO}_3$  can be selected as the ideal eluent relative to hydrochloric acid.

### The real seawater experiments

Uranium(VI) selectivity of PP-g-PO was evaluated by sorption experiments in real seawater. As shown in Fig. 5, the sorption selectivity of PP-g-PO was calculated to be 38.4%, which was much higher than that for vanadium(V) (about 2.5 times). The result indicated that oxime can significantly improve the adsorption selectivity for uranium(VI) compared with amidoxime. Furthermore, it also showed good binding selectivity for uranium(VI) against other cations, such as  $\text{Fe}^{3+}$ ,  $\text{Cu}^{2+}$ ,  $\text{Co}^{2+}$ ,  $\text{Ni}^{2+}$ ,  $\text{Zn}^{2+}$ , etc., which attributed to the strong affinity between oxime and uranium(VI). In addition, the positive charged sorbent will attract negative uranyl complex by coulombic interaction while repel cations. The similar results about the selectivity of oxime toward uranium(VI) and other ions have been reported in our previous study [26]. The results demonstrate that polyoxime

modified sorbents have much better selectivity than polyaminoxime modified materials.

### Antibacterial assay

The antibacterial properties of the materials were examined by comparing the amount of bacteria adhering to the surface of the sorbents for 24 h. As shown in Fig. 6A, C, the number of *E. coli* and *S. aureus* on PP non-woven fabrics was relatively high after 24 h of incubation, while there was almost no bacterium on PP-g-PO (Fig. 6B, D). This result indicates that the guanidine-modified polypropylene non-woven fabric has an effective antibacterial adhesion property.

The bactericidal properties of the material were further investigated by coating method. As shown in Fig. 7, the bacteria treated with the unmodified polypropylene non-woven fabric grew into a large number of colonies on the agar medium. However, the bacterial colonies treated by PP-g-PO were significantly reduced, indicating that PP-g-PO can be effectively sterilized and can be used in real seawater experiments in the future.

### Possible sorption mechanism

The possible sorption mechanism was investigated with the XPS spectra of PP-g-PO before and after uranium(VI) adsorption. After adsorption, the two sharp peaks at 393.60 eV and 382.95 eV belong to U 4f<sub>5/2</sub> and U 4f<sub>7/2</sub> (Fig. 8A, trace b), respectively, which proved that lots of uranium(VI) was combined with PP-g-PO.

The O 1s peak of PP-g-PO is located at 533.68 eV (Fig. 1C) assigned to the C(N)–O–H, while the peak was divided into two peaks at 534.51 and 533.30 eV (Fig. 8B,

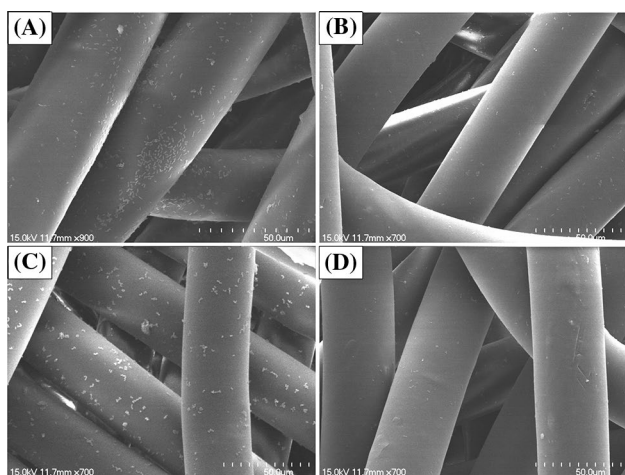


**Fig. 6** SEM images of *E. coli* on the **A** PP non-woven and **B** PP-g-PO for 24 h, and *S. aureus* on the **C** PP non-woven and **D** PP-g-PO for 24 h

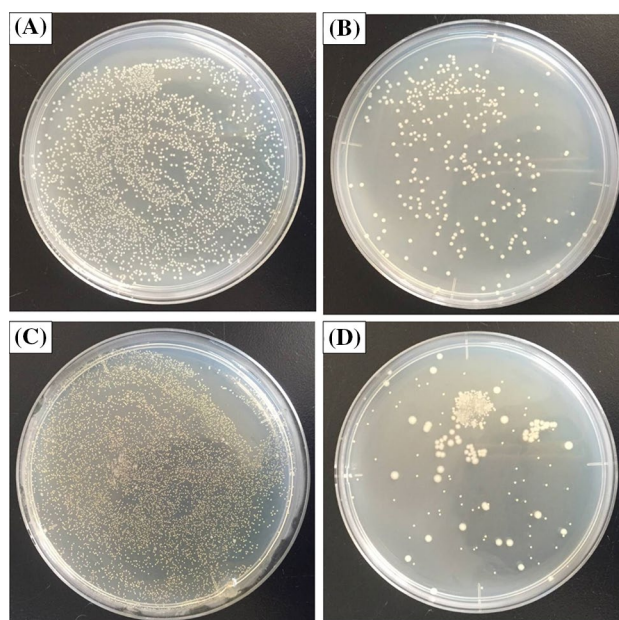


**Fig. 7** Photographs of agar plates corresponding to the *E. coli* suspension recovered from **A** PP nonwoven, **B** PP-g-PO, and *S. aureus* on the **C** PP non-woven and **D** PP-g-PO

and Table S2, Supporting Information) after adsorption. The appearance of 534.51 eV is owing to the bond of oxime with uranium(VI) via complexation, leading to a higher binding energy [40, 41]. However, the peak at 533.30 eV may be due to the covalent bonds formed between hydroxyl (-OH) and uranium(VI) [42]. The O 1s peaks of carbonyl groups (C=O) shifted to lower binding energy, which was perhaps ascribed to the interaction between C=O and uranium via covalent bond. In the case of N 1s, C=N and N–H both shifted to higher binding energy, which possibly ascribed to coordination between amino/oxime and uranium(VI) [26]. The XPS data indicated that oxime, amino, hydroxyl as well as carbonyl groups on PP-g-PO all contributed to the sorption.

### Conclusions

In summary, we demonstrate a new sorbent for highly selective recovery uranium(VI) from seawater with antibiofouling property. The successful synthesis of materials was verified by FT-IR, XPS, FE-SEM, EDX, and water contact angles. The sorption in real seawater validated that the adsorbent held outstanding selectivity for uranium(VI) over other common cations in seawater, especially vanadium(V). The antibacterial assay indicated the bifunctional polypropylene nonwoven fabric has good antibacterial properties against *E. coli* and *S. aureus*. The adsorption could reach equilibrium within 4 h with a maximum adsorption capacity of 120 mg/g

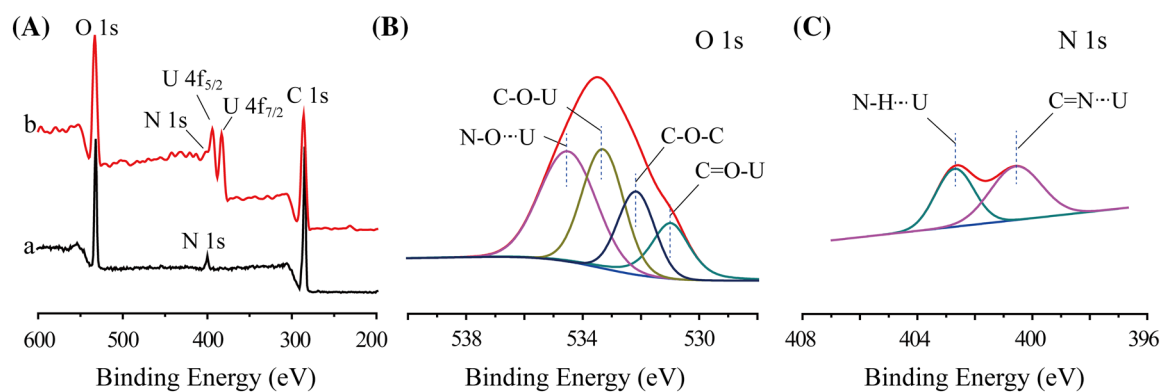


**Fig. 8** A XPS survey scan of (a) PP-g-PO, (b) PP-g-PO with uranium(VI); **B** O 1s peak of PP-g-PO with uranium(VI); and **C** N 1s peak of PP-g-PO with uranium(VI)

from Langmuir model at 298.15 K and pH  $8.0 \pm 0.1$ . Furthermore, no significant decrease in sorption efficiency was observed following five sorption–desorption cycles using  $\text{KHCO}_3$  solution as an eluent. The sorption mechanism involved the interaction of multiple groups including oxime, amino, hydroxyl and carbonyl groups with uranyl ions.

To the best of our knowledge, oxime and guanidine bifunctional adsorbent is used to adsorb uranium from seawater for the first time. The adsorbent showed higher selectivity toward uranium(VI) over vanadium(V) compared with guanidine and amidoxime co-functionalized fabric [25]. Furthermore, the material has excellent antibacterial activity and operability in comparison with polyoxime-functionalized magnetic nanoparticles [22]. This study demonstrates that PP-g-PO can be a hopeful material for the extraction of uranium from seawater.

**Acknowledgements** This work is supported by Natural Science Foundation of China (U1867206), a Project Funded by the Priority Academic Program Development of Jiangsu Higher Education Institutions (PAPD), and Jiangsu Key Laboratory of Radiation Medicine and Protection.

### Compliance with ethical standards

**Conflict of interest** The authors declare that they have no conflict of interest.

### References

- Davies RV, Kennedy J, McIlroy RW, Spence R, Hill KM (1964) Extraction of uranium from sea water. *Nature* 203:1110–1115
- Abney CW, Mayes RT, Saito T, Dai S (2017) Materials for the recovery of uranium from seawater. *Chem Rev* 117:13935–14013
- Liu C, Hsu PC, Xie J, Zhao J, Wu T, Wang H, Liu W, Zhang J, Chu S, Cui Y (2017) A half-wave rectified alternating current electrochemical method for uranium extraction from seawater. *Nat Energy* 2:17007
- Macfarlane AM (2011) The overlooked back end of the nuclear fuel cycle. *Science* 333:1225–1226
- Luo W, Xiao G, Tian F, Richardson JJ, Wang Y, Zhou J, Guo J, Liao X, Shi B (2019) Engineering robust metal-phenolic network membranes for uranium extraction from seawater. *Energy Environ Sci* 12:607–614
- Zhu J, Liu Q, Liu J, Chen R, Zhang H, Yu J, Zhang M, Li R, Wang J (2018) Novel ion-imprinted carbon material induced by hyperaccumulation pathway for the selective capture of uranium. *ACS Appl Mater Interfaces* 10:28877–28886
- Husnain SM, Kim HJ, Um W, Chang YY, Chang YS (2017) Superparamagnetic adsorbent based on phosphonate grafted mesoporous carbon for uranium removal. *Ind Eng Chem Res* 56:9821–9830
- Singhal P, Jha SK, Pandey SP, Neogy S (2017) Rapid extraction of uranium from sea water using  $\text{Fe}_3\text{O}_4$  and humic acid coated  $\text{Fe}_3\text{O}_4$  nanoparticles. *J Hazard Mater* 335:152–161
- Qian Y, Yuan Y, Wang H, Liu H, Zhang J, Shi S, Guo Z, Wang N (2018) Highly efficient uranium adsorption by salicyldoxime/polydopamine graphene oxide nanocomposites. *J Mater Chem A* 6:24676–24685
- Yuan Y, Yang Y, Ma X, Meng Q, Wang L, Zhao S, Zhu G (2018) Molecularly imprinted porous aromatic frameworks and their composite components for selective extraction of uranium ions. *Adv Mater* 30:1706507
- Sun Q, Aguila B, Earl LD, Abney CW, Wojtas L, Thallapally PK, Ma S (2018) Covalent organic frameworks as a decorating platform for utilization and affinity enhancement of chelating sites for radionuclide sequestration. *Adv Mater* 30:1705479
- Das S, Brown S, Mayes RT, Janke CJ, Tsouris C, Kuo LJ, Gill G, Dai S (2016) Novel poly(imide dioxime) sorbents: development and testing for enhanced extraction of uranium from natural seawater. *Chem Eng J* 298:125–135
- Wu F, Ning P, Ye G, Sun T, Wang Z, Yang S, Wang W, Huo X, Lu Y, Chen J (2017) Performance and mechanism of uranium adsorption from seawater to poly(dopamine)-inspired sorbents. *Environ Sci Technol* 51:4606–4614
- Das S, Mayes RT, Oyola Y, Janke CJ, Kuo LJ, Gill GA, Wood J, Dai S (2015) Extracting uranium from seawater: promising ai series adsorbents. *Ind Eng Chem Res* 55:4103–4109
- Wang D, Song J, Wen J, Yuan Y, Liu Z, Lin S, Wang H, Wang H, Zhao S, Zhao X, Fang M, Lei M, Li B, Wang N, Wang X, Wu H (2018) Significantly enhanced uranium extraction from seawater with mass produced fully amidoximated nanofiber adsorbent. *Adv Energy Mater* 8:1802607



16. Singhal P, Jha SK, Vats BG, Ghosh HN (2017) Electron-Transfer-Mediated uranium detection using quasi-type II core-shell quantum dots: insight into mechanistic pathways. *Langmuir* 33:8114–8122
17. Singhal P, Pulhani V (2019) Effect of ligand concentration, dilution, and excitation wavelength on the emission properties of CdSe/CdS core shell quantum dots and their implication on detection of uranium. *ChemistrySelect* 4:4528–4537
18. Hua M, Yang S, Ma J, He W, Kuang L, Hua D (2018) Highly selective and sensitive determination of uranyl ion by the probe of CdTe quantum dot with a specific size. *Talanta* 190:278–283
19. Wen J, Huang Z, Hu S, Li S, Li W, Wang X (2016) Aggregation-induced emission active tetraphenylethene-based sensor for uranyl ion detection. *J Hazard Mater* 318:363–370
20. Xiang Y, Wang Z, Xing H, Wong N, Lu Y (2010) Label-free fluorescent functional DNA sensors using unmodified DNA: a vacant site approach. *Anal Chem* 82:4122–4129
21. Shu X, Wang Y, Zhang S, Huang L, Wang S, Hua D (2015) Determination of trace uranyl ion by thermoresponsive porphyrin-terminated polymeric sensor. *Talanta* 131:198–204
22. Brown S, Yue Y, Kuo LJ, Mehio N, Li M, Gill G, Tsouris C, Mayes RT, Saito T, Dai S (2016) Uranium adsorbent fibers prepared by atom-transfer radical polymerization (ATRP) from poly(vinyl chloride)-*co*-chlorinated poly(vinyl chloride) (PVC-*co*-CPVC) fiber. *Ind Eng Chem Res* 55:4139–4148
23. Ivanov AS, Leggett CJ, Parker BF, Zhang Z, Arnold J, Dai S, Abney CW, Bryantsev VS, Rao L (2017) Origin of the unusually strong and selective binding of vanadium by polyamidoximes in seawater. *Nat Commun* 8:1560
24. Leggett CJ, Parker BF, Teat SJ, Zhang Z, Dau PD, Lukens WW, Peterson SM, Ajp C, Warner MG, Gibson JK (2016) Structural and spectroscopic studies of a rare non-oxido V(V) complex crystallized from aqueous solution. *Chem Sci* 7:2775–2786
25. Vukovic S, Hay BP (2013) De Novo structure-based design of bis-amidoxime uranophiles. *Inorg Chem* 52:7805–7810
26. Xu M, Han X, Hua D, Xu M, Han X, Hua D, Xu M, Han X, Hua D, Xu M (2017) Polyoxime-functionalized magnetic nanoparticles for uranium adsorption with high selectivity over vanadium. *J Mater Chem A* 5:12278–12284
27. Hu J, Ma H, Xing Z, Liu X, Xu L, Li R, Lin C, Wang M, Li J, Wu G (2015) Preparation of amidoximated ultrahigh molecular weight polyethylene fiber by radiation grafting and uranium adsorption test. *Ind Eng Chem Res* 55:4118–4124
28. Park J, Gill GA, Strivens JE, Kuo LJ, Jeters R, Avila A, Wood J, Schlafer NJ, Janke CJ, Miller EA (2016) Effect of biofouling on the performance of amidoxime-based polymeric uranium adsorbents. *Ind Eng Chem Res* 55:4328–4338
29. Zhang H, Zhang L, Han X, Kuang L, Hua D (2018) Guanidine and amidoxime cofunctionalized polypropylene nonwoven fabric for potential uranium seawater extraction with antifouling property. *Ind Eng Chem Res* 57:1662–1670
30. Zhou ZX, Wei DF, Guan Y, Zheng AN, Zhong JJ (2010) Damage of *Escherichia coli* membrane by bactericidal agent polyhexamethylene guanidine hydrochloride: micrographic evidences. *J Appl Microbiol* 108:898–907
31. Wen J, Li Q, Li H, Chen M, Hu S, Cheng H (2018) Nano-TiO<sub>2</sub> imparts amidoximated wool fibers with good antibacterial activity and adsorption capacity for uranium(VI) recovery. *Ind Eng Chem Res* 57:1826–1833
32. Zhang F, Zhang H, Chen R, Liu Q, Liu J, Wang C, Sun Z, Wang J (2019) Mussel-inspired antifouling magnetic activated carbon for uranium recovery from simulated seawater. *J Colloid Interface Sci* 534:172–182
33. Zhang S, Zhao XS, Li B, Bai CY, Li Y, Wang L, Wen R, Zhang MC, Ma LJ, Li SJ (2016) “Stereoscopic” 2D super-microporous phosphazene-based covalent organic framework: design, synthesis and selective sorption towards uranium at high acidic condition. *J Hazard Mater* 314:95–104
34. Li P, Poon YF, Li WF, Zhu HY, Yeap SH, Cao Y, Qi XB, Zhou CC, Lamrani M, Beuerman RW, Kang ET, Mu YG, Li CM, Chang MW, Leong SSJ (2011) A polycationic antimicrobial and biocompatible hydrogel with microbe membrane suctioning ability. *Nat Mater* 10:149–156
35. Tian B, Wang XY, Zhang LN, Shi FN, Zhang Y, Li SX (2016) Preparation of PVDF anionic exchange membrane by chemical grafting of GMA onto PVDF macromolecule. *Solid State Ionics* 293:56–63
36. Xin Z, Du S, Zhao C, Chen H, Sun M, Yan S, Luan S, Yin J (2016) Antibacterial performance of polypropylene nonwoven fabric wound dressing surfaces containing passive and active components. *Appl Surf Sci* 365:99–107
37. Yang S, Qian J, Kuang L, Hua D (2017) Ion-imprinted mesoporous silica for selective removal of uranium from highly acidic and radioactive effluent. *ACS Appl Mater Interfaces* 9:29337–29344
38. Pan HB, Wai CM, Kuo LJ, Gill G, Tian G, Rao L, Das S, Mayes RT, Janke CJ (2017) Bicarbonate elution of uranium from amidoxime-based polymer adsorbents for sequestering uranium from seawater. *Chemistryselect* 2:3769–3774
39. Chavan SP, Soni P (2004) A facile deprotection of oximes using glyoxylic acid in an aqueous medium. *Tetrahedron Lett* 45:3161–3162
40. Song W, Liu M, Hu R, Tan X, Li J (2014) Water-soluble polyacrylamide coated-Fe<sub>3</sub>O<sub>4</sub> magnetic composites for high-efficient enrichment of U(VI) from radioactive wastewater. *Chem Eng J* 246:268–276
41. Zhang M, Gao Q, Yang C, Pang LJ, Wang HL, Li H, Li R, Xu L, Xing Z, Hu J (2016) Preparation of amidoxime-based nylon 66 fibers for removing uranium from low concentration aqueous solutions and simulated nuclear industry effluents. *Ind Eng Chem Res* 55:10523–10532
42. Sun Y, Wu ZY, Wang X, Ding C, Cheng W, Yu SH, Wang X (2016) Macroscopic and microscopic investigation of U(VI) and Eu(III) adsorption on bacterium-derived carbon nanofibers. *Environ Sci Technol* 50:4459

**Publisher's Note** Springer Nature remains neutral with regard to jurisdictional claims in published maps and institutional affiliations.

## Affiliations

Sen Yang<sup>1</sup> · Guoxun Ji<sup>2</sup> · Suya Cai<sup>1</sup> · Meiyu Xu<sup>1</sup> · Daoben Hua<sup>1,3</sup> 

✉ Daoben Hua  
dbhua\_lab@suda.edu.cn

<sup>3</sup> Collaborative Innovation Center of Radiological Medicine of Jiangsu Higher Education Institutions, Suzhou 215123, China

<sup>1</sup> State Key Laboratory of Radiation Medicine and Protection, School for Radiological and Interdisciplinary Sciences (RAD-X), Soochow University, Suzhou 215123, China

<sup>2</sup> Xi'an Research Institution of Hi-Tech, Xi'an 710025, China